Liquid Crystals
Publication details, including instructions for authors and subscription information:
http://www.informaworld.com/smpp/title~content=t713926090

On the analogy between the field-induced and flow-induced deformations in nematic liquid crystals

Grzegorz Derfel

Online publication date: 06 August 2010

To cite this Article Derfel, Grzegorz(1998) 'On the analogy between the field-induced and flow-induced deformations in nematic liquid crystals', Liquid Crystals, 24: 6, 829 — 834
To link to this Article: DOI: 10.1080/026782998206641
URL: http://dx.doi.org/10.1080/026782998206641

LIQUID CRYSTALS, 1998, VOL. 24, NO. 6, 829–834

On the analogy between the field-induced and flow-induced deformations in nematic liquid crystals

by GRZEGORZ DERFEL

Institute of Physics, Technical University of Łódź, ul. Wólczańska 223, 93-005 Łódź, Poland

(*Received 27 May 1997; in final form 16 December 1997; accepted 17 January 1998*)

The analogy between the field-induced and flow-induced deformations of nematic liquid crystals is summarized. The threshold onset of the deformation occurring under rigid boundary conditions, the unwinding of the helical axis in a chiral nematic material, and the saturation threshold appearing for weak anchoring are described as examples of analogous phenomena which take place both in external fields and during shear flow. The analogy has allowed prediction of a new threshold effect possible in a sheared, weakly anchored nematic. The description of this effect is supported by numerical calculations. Stability analysis was also performed.

1. Introduction

From the macroscopic point of view, an equilibrium state of a nematic liquid crystal is characterized by a director field $\mathbf{n}(\mathbf{r})$. It is well known since the early stages of the study of liquid crystals that the director distribution can be easily influenced by external fields, flow and surface interactions [1]. In this paper, the analogy between the orienting effects induced by an external magnetic field and by flow of the liquid crystal material is discussed. Only the static deformations of defect-free structures are taken into account. For the sake of clarity, the simplest cases of a chiral nematic subjected to a magnetic field or to simple shear flow are considered. The surface interactions, which determine the boundary conditions, are taken into account in all cases. The properties of the torques influencing the director field are described in § 2. The results illustrating the above mentioned analogy are briefly reviewed in § 3 and 4. In § 5, this picture is completed by analysis of one particular new case, namely the deformation of a weakly anchored nematic oriented at a certain special angle and subjected to shear flow. This case reveals the threshold character and is predicted from the analogy to the deformation taking place in an external field.

In the following, the chiral nematic liquid crystal is characterized by diamagnetic anisotropy $\Delta\chi$, elastic constants k_{11}, k_{22}, k_{33}, undistorted pitch P_0 and Leslie viscosity coefficients α_i, ($i = 1$–6).

2. The torques

The torques acting on the director, referred to unit volume of the nematic liquid crystal, are given by the textbook formulae [1]. In real samples, the director distribution is affected by torques of two or more types at the same time. In this section however, the torque of each type is described independently.

In the case of a magnetic field of strength $\mathbf{H}$, the torque is

$$\Gamma_{\text{magnetic}} = \Delta\chi(\mathbf{n}\ \ \mathbf{H})(\mathbf{n} \times \mathbf{H}). \tag{1}$$

It vanishes, if $\mathbf{n} \| \mathbf{H}$ or $\mathbf{n} \perp \mathbf{H}$. Both configurations may correspond either to the stable or to the unstable equilibrium, depending on the sign of the diamagnetic anisotropy $\Delta\chi$.

In the case of flow, the torque is due to the coupling between the director and the velocity gradient. It is determined by the velocity field $\mathbf{v}(\mathbf{r})$ and is described by a somewhat more complex formula

$$\Gamma_{\text{viscous}} = \mathbf{n} \times (\gamma_1 \mathbf{N} + \gamma_2 \mathbf{d}\ \ \mathbf{n}) \tag{2}$$

where $\gamma_1 = \alpha_3 - \alpha_2$, $\gamma_2 = \alpha_3 + \alpha_2$, $\mathbf{N} = \dot{\mathbf{n}} - \omega \times \mathbf{n}$, $\omega = 1/2(\nabla \times \mathbf{v})$, and $\mathbf{d}$ is a symmetric part of the velocity gradient tensor which has components

$$d_{ij} = \frac{1}{2}\left(\frac{\partial v_i}{\partial x_j} + \frac{\partial v_j}{\partial x_i}\right).$$

The quantity $\gamma_1 \mathbf{N} + \gamma_2 \mathbf{d}\ \ \mathbf{n} \equiv \mathbf{U}$ represents a viscous part of the molecular field. In the static cases considered in this paper, $\dot{\mathbf{n}} = 0$. The viscous torque vanishes if $\mathbf{U} = 0$ or if $\mathbf{U} \| \mathbf{n}$. The former case becomes real if $\mathbf{n}$ is normal to the plane of shear, i.e. $\mathbf{n} \perp \mathbf{v}$ and $\mathbf{n} \perp \nabla \mathbf{v}$. The condition $\mathbf{U} \| \mathbf{n}$ corresponds to two distinct director orientations within the plane of shear, when the angle θ measured between $\mathbf{n}$ and $\mathbf{v}$ is equal to $+\theta_c$ or $-\theta_c$, where $\theta_c = \arctan(\alpha_3/\alpha_2)^{1/2}$. In the following, these two orientations will be distinguished by means of two versors denoted $\mathbf{c}^+$ and $\mathbf{c}^-$, respectively. They exist only for so-called 'flow aligning nematics', for which $\alpha_3/\alpha_2 > 0$. The orientation $\mathbf{c}^+$ corresponds to the stable equilibrium, whereas $\mathbf{c}^-$ is related to the unstable equilibrium. These two orientations are analogous to the states $\mathbf{n}\|\mathbf{H}$ and $\mathbf{n}\perp\mathbf{H}$ occurring for $\Delta\chi > 0$, respectively. In materials for which $\alpha_3/\alpha_2 < 0$, the only possibility of equilibrium in the shear flow appears if $\mathbf{n}$ is normal to the shear plane, since $\mathbf{U} = 0$. The condition $\mathbf{U} = 0$ corresponds to the trivial equilibrium $\mathbf{H} = 0$ in the magnetic case. If $\mathbf{U} \neq 0$, no equilibrium is realized. In the magnetic counterpart of this case, the field $\mathbf{H} \neq 0$ always leads to an equilibrium. This means that nematic liquid crystals are always 'field aligning'. The analogies mentioned in the following sections concern flow aligning nematics.

The boundary conditions are usually described by the Rapini–Papoular expression for the surface interaction energy

$$F_{\text{surface}} = -(W/2)(\mathbf{n}\ \ \mathbf{e})^2 \tag{3}$$

where W is the anchoring energy coefficient and $\mathbf{e}$ is the easy axis versor. The surface torque is therefore given by

$$\Gamma_{\text{surface}} = W(\mathbf{n}\ \ \mathbf{e})(\mathbf{n} \times \mathbf{e}) \tag{4}$$

and this vanishes if $\mathbf{n}\|\mathbf{e}$ or $\mathbf{n}\perp\mathbf{e}$ giving the stable and unstable equilibrium, respectively.

The torque per unit volume due to the curvature elasticity is determined by the formula

$$\Gamma_{\text{elastic}} = \mathbf{n} \times \mathbf{h}_e \tag{5}$$

where $\mathbf{h}_e$ is the elastic part of the molecular field, consisting of three parts

$$\mathbf{h}_e = \mathbf{h}_S + \mathbf{h}_T + \mathbf{h}_B \tag{6}$$

where

$$\begin{aligned} \mathbf{h}_S &= k_{11}\nabla(\nabla\ \ \mathbf{n}) \\ \mathbf{h}_T &= -k_{22}[\mathbf{A}(\nabla \times \mathbf{n}) + \nabla \times (\mathbf{A}\ \ \mathbf{n})] \\ \mathbf{h}_B &= k_{33}[\mathbf{B} \times (\nabla \times \mathbf{n}) + \nabla \times (\mathbf{n} \times \mathbf{B})] \end{aligned} \tag{7}$$

and

$$\begin{aligned} \mathbf{A} &= \mathbf{n}\ \ (\nabla \times \mathbf{n}) \\ \mathbf{B} &= \mathbf{n} \times (\nabla \times \mathbf{n}). \end{aligned}$$

This rather complex expression can be significantly simplified when the one-constant approximation ($k_{11} = k_{22} = k_{33} \equiv k$) is adopted:

$$\mathbf{h}_e = k\nabla^2\mathbf{n}. \tag{8}$$

In the absence of other torques, $\mathbf{n}\|\mathbf{h}_e$ and Γ_{elastic} vanish identically. The elastic torque vanishes also when $\mathbf{h}_e = 0$. In the equal elastic constants' approximation, the latter condition can be easily expressed as

$$\nabla^2\mathbf{n} = 0. \tag{9}$$

This is satisfied for instance at a uniform director field. In the examples discussed in this paper only uniform director distributions are considered as structures in which $\Gamma_{\text{elastic}} = 0$.

3. The threshold effects

In this section a uniform layer of thickness d placed parallel to the xy plane is considered. The rigid boundary orientations, identical on both plates, are determined by the easy axis versors $\mathbf{e}$. The layer is under the influence of the magnetic field $\mathbf{H}$, or it is subjected to the simple shear flow occurring under the action of a shear stress τ directed along the y axis. The plane of shear is parallel to the yz plane. In general, when the magnetic field is arbitrarily oriented with respect to the easy axis, the deformation starts at any field strength. The same applies for the shear flow deformation, which starts at any shear stress if the surface orientation is arbitrary. The threshold behaviour can take place in configurations for which the undistorted state $\mathbf{n}\|\mathbf{e}$ remains in equilibrium at any field strength or at any shear stress. This condition is necessary for the bifurcation of the stable states. The torque of each kind (e.g. magnetic, viscous, elastic or surface anchoring torque) vanishes in such states. This condition is not sufficient in trivial cases which remain stable and undeformed: for example, the configuration $\mathbf{H}\|\mathbf{e}$ (and $\Delta\chi > 0$) in the magnetic case, and the configuration with $\mathbf{e}\|\mathbf{c}^+$ in the flow case.

In the magnetic case $\mathbf{H}\perp\mathbf{e}$, the equilibrium uniform state $\mathbf{n}\|\mathbf{e}$ loses its stability above the threshold field and bifurcation of the stable states develops. For instance, in a planar cell with $\mathbf{e}\|y$ and subjected to the field $\mathbf{H}\|z$, the threshold value is given by

$$H_0 = (\pi/d)(k_{11}/\Delta\chi)^{1/2}. \tag{10}$$

An analogous effect can be predicted for the shear flow case, if $\mathbf{n}$ is confined within the shear plane and aligned initially along the $\mathbf{e}$ versor forming the angle $-\theta_c$ against the y axis ($\mathbf{e}\|\mathbf{c}^-$), [2, 3]. The threshold shear stress t_c, expressed in non-dimensional form, obtained by scaling with $k_{33}\pi^2/d^2$, is given by

$$t_c = \frac{(k_s + s)(s - r)}{2[s(1+s)]^{1/2}} \tag{11}$$

where $k_s = k_{11}/k_{33}$, $s = \alpha_3/\alpha_2$, $r = (\alpha_3 + \alpha_4 + \alpha_6)/(2\alpha_2)$, [3]. The unified description of both threshold phenomena can be given in terms of catastrophe theory [3, 4]. The cusp catastrophe is also adequate for both cases

[5]. The bifurcation of the equilibrium states is shown schematically in figure 1.

4. Chiral nematics

The most spectacular deformation of chiral nematics is the unwinding of the helical structure [6]. It occurs when the magnetic field is applied perpendicularly to the helix axis. The liquid crystal free from boundary constraints is considered for the sake of simplicity. In this case the structure deforms continuously. Its spatial period increases until the threshold magnetic field is achieved, [7]:

$$H_c = \frac{\pi^2}{P_0}\left(\frac{k_{22}}{\Delta\chi}\right)^{1/2}. \qquad (12)$$

As a result the nematic liquid crystal with $\mathbf{n}\|\mathbf{H}$ arises.

The shear flow can produce an analogous influence on the flow aligning chiral nematic when the helix axis is perpendicular to the velocity vector and to the velocity gradient [8]. An analogous critical shear rate u_c exists:

$$u_c = \frac{4\pi^4 k_{22}}{P_0^2 G^2} \qquad (13)$$

where

$$G = \int_{\theta_c-\pi}^{\theta_c} [\kappa - (\alpha_3 - \alpha_2)\theta + (\alpha_3 + \alpha_2)\sin\theta\cos\theta]^{1/2}\,\mathrm{d}\theta \qquad (14)$$

and

$$\kappa = (\alpha_3 - \alpha_2)\theta_c + (\alpha_3 + \alpha_2)\sin\theta_c\cos\theta_c \qquad (15)$$

above which the unwound nematic structure appears. The director is uniformly aligned in the plane of shear and makes the angle θ_c with the flow direction.

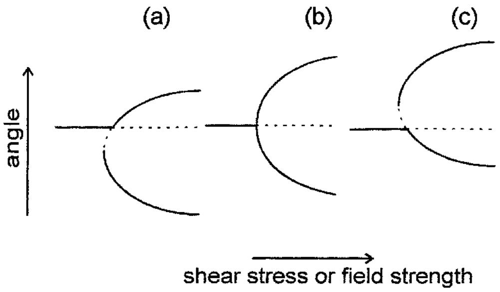

Figure 1. The bifurcation of equilibrium states due to the cusp catastrophe. In the magnetic case the curve (*b*) occurs for planar or homeotropic layers whereas the curves (*a*) and (*c*) occur for obliquely oriented layers. In the flow case, the curves (*a*), (*b*) and (*c*) appear sequentially for increasing values of *s*. Full lines are due to stable states, dotted lines to unstable states.

5. Weak anchoring

Under infinite or very strong anchoring conditions, the director at the boundaries remains undeformed regardless of the nature of the external forces. However if the anchoring is weak, the director field can be deformed not only in the bulk, but also at the boundary plates.

Let us consider a uniform nematic slab confined between two plates on which $\mathbf{e}\|y$ and subjected to the magnetic field $\mathbf{H}\|z$ [9, 10, 11]. The necessary condition for the threshold behaviour is fulfilled in two cases: $\mathbf{n}\|\mathbf{e}$ and $\mathbf{n}\perp\mathbf{e}$, since in both configurations the torques of each kind, exerted on the director in a uniform nematic, vanish simultaneously: $\Gamma_{\text{magnetic}}=0$, $\Gamma_{\text{elastic}}=0$, $\Gamma_{\text{surface}}=0$. In the absence of the field, or at sufficiently low fields, the state $\mathbf{n}\|\mathbf{e}$ is stable. This state loses its stability above a certain threshold H_1. New stable states due to the distorted director field appear. The configuration $\mathbf{n}\perp\mathbf{e}$ is unstable at low field, but it becomes stable above some other threshold field $H_2 > H_1$, when the layer is uniformly aligned along the field $\mathbf{n}\|\mathbf{H}$. Both thresholds depend on the anchoring energy and, in the one constant approximation, are given by the formulae [9]:

$$\frac{\pi H_1}{g H_0} = \cot\left(\frac{\pi H_1}{2H_0}\right) \qquad (16)$$

$$\frac{\pi H_2}{g H_0} = \coth\left(\frac{\pi H_2}{2H_0}\right) \qquad (17)$$

where H_0 is given by equation (10) and $g = W\,d/k_{11}$.

One can try to extend the analogy considered in this paper in order to find new effects in the case of shear flow. However in the case of shear flow, the analogy of the field induced behaviour is incomplete.

The viscous torque can vanish in the uniform layer if the director is oriented at the angle θ_c or $-\theta_c$, i.e. if $\mathbf{n}\|\mathbf{c}^+$ or $\mathbf{n}\|\mathbf{c}^-$. The surface torque vanishes if $\mathbf{n}\|\mathbf{e}$ or $\mathbf{n}\perp\mathbf{e}$. These conditions distinguish four equilibrium configurations: two with $\mathbf{n}\|\mathbf{e}$ and two with $\mathbf{n}\perp\mathbf{e}$.

The configuration ($\mathbf{n}\|\mathbf{e}$, $\mathbf{e}\|\mathbf{c}^+$) is stable at any shear stress. The structure ($\mathbf{n}\|\mathbf{e}$, $\mathbf{e}\|\mathbf{c}^-$) becomes deformed above the threshold stress as described in §3. The second threshold stress analogous to H_2 cannot exist for this structure, since the final orientation $\mathbf{n}\|\mathbf{c}^+$ is not perpendicular to $\mathbf{e}$, and Γ_{surface} remains different from zero.

The two structures with $\mathbf{n}\perp\mathbf{e}$ are obviously not stable at rest. They cannot be taken into account as the initial states and therefore no threshold onset of deformation can occur for them. The configuration ($\mathbf{n}\|\mathbf{c}^-$, $\mathbf{e}\perp\mathbf{c}^-$) is not stable at high stress either.

The last configuration ($\mathbf{n}\|\mathbf{c}^+$, $\mathbf{e}\|\mathbf{c}^+$) assures stability at sufficiently high stress and yields an opportunity for the upper threshold shear stress, above which the final structure $\mathbf{n}\|\mathbf{c}^+$ becomes stable. In the following, the stability of such a system is analysed and then a suitable example is calculated numerically.

5.1. *Stability analysis*

Let us consider the flow aligning nematic layer oriented by the particular boundary conditions at the angle $\theta_s = \theta_c + \pi/2$. The director does not come out of the plane of shear under these circumstances and its distribution can be described by only one angle $\theta(z)$. The complete form of the approach applied here was used earlier in ref. [3].

The distortion of the director field under the action of the shear stress is connected with the free energy due to the curvature elasticity and to the action of the viscous torque [3, 12]. Its value per unit area of the layer can be expressed in a form [3]

$$F = \frac{k_{33}}{2d}\int_{-1/2}^{1/2}(\sin^2\theta - k_s\cos^2\theta)\left(\frac{d\theta}{d\varsigma}\right)^2 d\varsigma + t\frac{k_{33}\pi^2}{d^2} \times \int_{-1/2}^{1/2}\left\{\theta - \frac{r-s}{(pr)^{1/2}}\arctan\left[\left(\frac{p}{r}\right)^{1/2}\tan\theta\right]\right\}d\varsigma - \frac{2k_{33}}{d}gk_s[\cos^2(\theta_b - \theta_s)] \tag{18}$$

where $p = r - s - 1$, $\varsigma = z/d$ and θ_b determines the director orientation at $z = \pm d/2$.

The stability in the $\mathbf{n}\|\mathbf{c}^+$ structure, with respect to small perturbations, is investigated. The perturbed director distribution is assumed in a form

$$\theta(\zeta) = \theta_c + \xi\cos(\pi\varsigma) + \psi. \tag{19}$$

Therefore F is analysed as a function of two variables ξ and ψ. The angle ξ measures the amplitude of the deformation, and the angle ψ measures the director deviation at the boundaries. The real form of the $\theta(\varsigma)$ dependence differs from the cosinusoidal shape assumed by equation (19). Therefore the analysis has only qualitative character. The unperturbed state $\theta(\varsigma) = \theta_c$ is related to equilibrium, since $\partial F/\partial\xi|_{\xi=0,\psi=0} = 0$ and $\partial F/\partial\psi|_{\xi=0,\psi=0} = 0$ at any shear stress. The state $\xi = 0$, $\psi = 0$ is stable, provided that

$$\partial^2 F/\partial\xi^2|_{\xi=0,\psi=0} > 0 \tag{20}$$

and

$$\det\begin{bmatrix} \dfrac{\partial^2 F}{\partial\xi^2} & \dfrac{\partial^2 F}{\partial\xi\partial\psi} \\ \dfrac{\partial^2 F}{\partial\xi\partial\psi} & \dfrac{\partial^2 F}{\partial\psi^2}\end{bmatrix}_{\xi=0,\psi=0} > 0 \tag{21}$$

which lead to two inequalities:

$$\frac{k_s + s}{1+s} - t\frac{2s^{1/2}}{r-s} > 0 \tag{22}$$

$$t^2(\pi^2 - 8)\frac{2s}{(r-s)^2} + t\left(4gk_s - \pi^2\frac{k_s+s}{1+s}\right)\frac{s^{1/2}}{r-s} - 2gk_s\frac{k_s+s}{1+s} > 0. \tag{23}$$

The above conditions are satisfied if the shear stress exceeds the threshold value t_2. For instance, its numerical value is $t_2 = 6{\cdot}12$ for the material constants: $k_s = 0{\cdot}833$, $s = 0{\cdot}01$, $r = -0{\cdot}2$, which give $\theta_c = 0{\cdot}09968$ and for the anchoring parameter $g = 5$.

5.2. *Numerical results*

The threshold behaviour predicted above is confirmed by the numerical solution of the balance of torques equations. In figure 2, the midplane angle θ_m and the boundary angle θ_b are plotted against the shear stress t. At high stress, the $\theta_m(t)$ curve approaches the θ_c value almost tangentially. The threshold effect is however evident from the $\theta_b(t)$ plot, which ends at about $t = 7{\cdot}8$. In order to show the peculiar character of the behaviour, the $\theta_b(t)$ dependence for $\theta_s = \pi/2$ is plotted for comparison. The development of the deformation with increasing t is illustrated in figure 3, where the profiles $\theta(\varsigma)$ are shown. The profiles for high stresses are flatter than that postulated by means of equation (19), which may be the reason for the quantitative discrepancy between the threshold values obtained in the two ways. The high stress structure is uniform with $\theta(\varsigma) = \theta_c$. Analogy with the magnetic case is evident from figure 4,

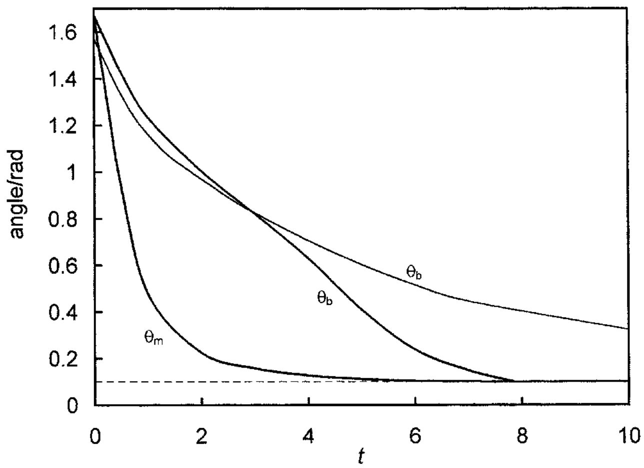

Figure 2. The mid-plane angle θ_m and the boundary angle θ_b as functions of the reduced shear stress t. Full lines are due to stable states, the dashed line to the unstable state ($\mathbf{n}\|\mathbf{c}^+$, $\mathbf{e}\perp\mathbf{c}^+$), and the thin line illustrates the $\theta_b(t)$ dependence of the homeotropic layer.

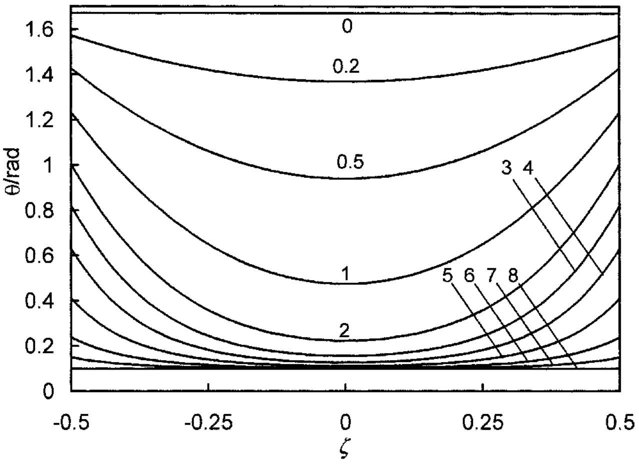

Figure 3. The director profiles $\theta(\varsigma)$ for various shear stresses (indicated for each curve).

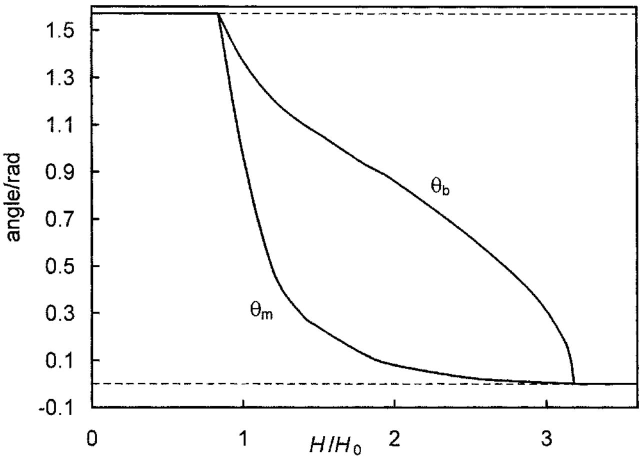

Figure 4. The mid-plane angle θ_m and the boundary angle θ_b as functions of the reduced magnetic field H/H_0 calculated for the homeotropic layer; $k_s = 0{\cdot}833$, $g = 5$. Full lines are due to stable states, dashed lines to unstable states.

where the deformation of the weakly anchored homeotropic layer induced by the magnetic field parallel to the plates is illustrated by numerical results.

6. Summary

In the present paper, the analogy between the field induced and the shear flow induced deformations has been illustrated. The simple geometry of the cases considered made it possible to reveal the similarities clearly, and a new effect was predicted on the basis of this analogy. Three examples of analogous behaviour have been presented:

(i) Deformations of the nematic layer in the external field and in shear flow possess threshold character.
(ii) Unwinding of the helical axis occurs both in the external field and in shear flow.
(iii) Weakly anchored nematics achieve the saturated deformation above some critical field strength and above some critical shear stress.

The deformations caused by the flow are more complex than those induced by the external fields.

In the magnetic case, two director orientations can be realized, depending on the sign of diamagnetic anisotropy: parallel or pependicular to the field vector **H**. The magnetic torque vanishes in these two orientations. Therefore there are two uniform director distributions, one perpendicular to the other, in which $\Gamma_{\text{magnetic}} = 0$, $\Gamma_{\text{elastic}} = 0$ and $\Gamma_{\text{surface}} = 0$ simultaneously (provided that the surface anchoring energy is determined by **n e**).

In the shear flow case, the equilibrium is realized in two uniform orientations determined by the versors $\mathbf{c}^+$ and $\mathbf{c}^-$. Their directions can vary continuously, depending on the material constants α_2 and α_3. The angle between the orientations $\mathbf{c}^+$ and $\mathbf{c}^-$ at which the viscous torque vanishes is equal to $2\theta_c$, which is smaller than $\pi/2$ and is temperature dependent. The torques Γ_{viscous}, Γ_{elastic} and Γ_{surface} can therefore vanish simultaneously only at one of the configurations $\mathbf{c}^+$ or $\mathbf{c}^-$. These features of the viscous torque lead to a rich variety of phenomena observed in flowing nematics. Even more dramatic evidence of the significance of the material constants for the character of the influence of the flow is the tumbling effect of non-flow aligning nematics, due to the non-vanishing viscous torque.

The surface orientation angles equal to θ_c or $\theta_c + \pi/2$, although very special, can be achieved experimentally by chemical treatment and rubbing techniques [13] which can produce the entire range of tilt angles from planar to homeotropic.

7. Conclusions

The analogy ascertained in this paper concerns static cases of one-dimensional deformations, but one can try to extend this analogy to dynamic phenomena and to two-dimensional deformations. This idea might lead to some new experimental and theoretical results. For instance, two possible effects can be taken into consideration:

(i) During the onset of the field induced transition, a transient backflow effect takes place [14]. An analogous phenomenon might be expected in the shear flow case. The transient director reorientation could then influence the velocity profile of the nematic by superimposing some kind of backflow on the shear induced flow.
(ii) In nematic liquid crystals possessing extremely high elastic anisotropy, the deformations caused

by the magnetic field take form of periodic patterns [15]. An analogous effect induced by shear flow is plausible for this class of nematics.

References

[1] De Gennes, P. G., 1974, *The Physics of Liquid Crystals* (Oxford: Clarendon Press).

[2] Currie, P. K., and Macsithigh, G. P., 1979, *Q. J. Mech. appl. Math.*, **32,** 499.

[3] Derfel, G., 1989, *Liq. Cryst.*, **6,** 709.

[4] Derfel, G., 1988, *Liq. Cryst.*, **3,** 1411.

[5] Gilmore, R., 1981, *Catastrophe Theory for Scientists and Engineers* (J. Wiley).

[6] Durand, G., Leger, L., Rondelez, F., and Veyssie, M., 1969, *Phys. Rev. Lett.*, **22,** 227.

[7] De Gennes, P. G., 1968, *Solid State Commun.*, **6,** 163.

[8] Derfel, G., 1983, *Mol. Cryst. liq. Cryst. Lett.*, **92,** 41.

[9] Nehring, J., Kmetz, A. R., and Scheffer, T. J., 1976, *J. appl. Phys.*, **47,** 850.

[10] Derfel, G., 1991, *Liq. Cryst.*, **10,** 29.

[11] Derfel, G., 1994, *Liq. Cryst.*, **17,** 429.

[12] Derfel, G., 1991, *Liq. Cryst.*, **10,** 647.

[13] Filas, R. W., and Patel, J. S., 1987, *Appl. Phys. Lett.*, **50,** 1426.

[14] Pierański, P., Brochard, F., and Guyon, E., 1973, *J. de Physique.*, **34,** 35.

[15] Lonberg, F., and Meyer, R. B., 1985, *Phys. Rev. Lett.*, **55,** 718.